Chem Biol Drug Des 2014; **84:** 108–115

Research Article

In vitro Evaluation of Doxorubicin-Incorporated Magnetic Albumin Nanospheres

Ayça Zeybek[1], Gülşah Şanlı-Mohamed[1], Güliz Ak[2], Habibe Yılmaz[2] and Şenay H. Şanlıer[2,*]

[1]Department of Chemistry, Faculty of Science, İzmir Institute of Technology, 35430 Urla, İzmir, Turkey
[2]Department of Biochemistry, Faculty of Science, Ege University, 35100 Bornova, Izmir, Turkey
**Corresponding author: Şenay H. Şanlıer, senay.sanlier@ege.edu.tr*

Magnetic albumin nanospheres that incorporate doxorubicin (M-DOX-BSA-NPs) were prepared previously by our research group to develop magnetically responsive drug carrier system. This nanocarrier was synthesized as a drug delivery system for targeted chemotherapy. In this work, cytotoxic effects of doxorubicin (DOX)-loaded/unloaded or magnetic/non-magnetic nanoparticles and free DOX against PC-3 cells and A549 cells were determined with the MTT test and the results were compared with each other. DOX-loaded magnetic albumin nanospheres (M-DOX-BSA-NPs) were found more cytotoxic than other formulations. The quantitative data obtained from flow cytometry analysis further verified the higher targeting and killing ability of M-DOX-BSA-NPs than free DOX on both of the cancer cell lines. Additionally, the results of cell cycle analysis have showed that M-DOX-BSA-NPs affected G1 and G2 phases. Finally, cell images were obtained using spin-disk confocal microscopy, and cellular uptake of M-DOX-BSA-NPs was visualized. The findings of this study suggest that M-DOX-BSA-NPs represent a potential doxorubicin delivery system for targeted drug transport into prostate and lung cancer cells.

Key words: A549 cell line, apoptosis, doxorubicin, magnetic albumin nanoparticle, PC3 cell line, targeted drug delivery

Received 24 September 2013, revised 19 November 2013 and accepted for publication 29 January 2014

In the last two decades, a number of nanoparticle-based therapeutic and diagnostic agents have been developed for the treatment of cancer (1). Nanoparticles made of albumin, which is a plasma protein, offer several specific advantages: they are non-toxic, non-antigenic, biodegradable, easy to prepare, reproducible, and well tolerated (2). There are human serum albumin-based particle formulations on the market such as Albunex™ and Abraxane™.

Doxorubicin (DOX) is the best known and most widely used member of the anthracycline antibiotic group of anticancer agents (3). DOX has a number of undesirable side-effects such as nausea, vomiting, hair loss, cardiotoxicity, and myelosuppression, which leads to a very narrow therapeutic index (4). Its mode of action is complex and not completely understood, but it is believed to interact with cell DNA by intercalation and subsequent inhibition of biosynthesis (5).

Nanoparticles, using both passive and active targeting strategies, can enhance the intracellular accumulation of drugs in cancer cells while avoiding toxicity in normal cells (6). Magnetic drug targeting ensures the concentration of drugs at a defined target site with the aid of a magnetic field. Typically, magnetic compound is injected through the artery supplying the tumor tissue in the presence of an external magnetic field with sufficient field strength and gradient to retain the carrier at the target site (7). Ferrimagnetic magnetite (Fe_3O_4) is suitable and biocompatible for *in vivo* applications as cell homeostasis is well controlled by iron uptake, excretion, and storage, and the iron excess is efficiently cleared from the body (8).

The purpose of this study was to evaluate the *in vitro* cytotoxicity effect of doxorubicin-loaded magnetic albumin nanospheres which were developed previously by our research group (5), against prostate and lung cancer cell lines. For this purpose, cell viability tests and apoptosis rate analysis were carried out, and cell images were visualized using optical and spin-disk confocal microscopy.

Methods and Materials

Materials

Bovine serum albumin (BSA) was purchased from Sigma-Aldrich Chemical co. (St. Louis, MO, USA), glutaraldehyde was obtained from Merck Chemical Co. (Darmstadt, Germany), and doxorubicin (DOX) was supplied from Med-Ilac (Istanbul, Turkey). All the other reagents were analytical grade. For cell culture studies, Roswell Park Memorial Institute-1640 (RPMI-1640) growth medium, Dulbecco's modified Eagle's medium (DMEM) growth medium, fetal bovine serum (FBS), and gentamicin sulfate were obtained from Gibco, BRL (New York, NY, USA). Dimethyl sulfoxide (DMSO), trypan blue dye, and MTT reagent were purchased

 doi: 10.1111/cbdd.12300

from Sigma-Aldrich Chemical co. Phosphate-buffered saline (PBS) was supplied from Invitrogen (Carlsbad, CA, USA). Annexin V apoptosis detection kit I was purchased from BD Pharmingen (SanDiego, CA, USA). Absolute ethanol was purchased from AppliChem GmbH (Darmstadt, Germany).

Preparation of doxorubicin-incorporated magnetic albumin nanospheres

Doxorubicin-incorporated magnetic albumin nanospheres (M-DOX-BSA-NPs) were developed according to the method described in our previous study (5). Briefly, doxorubicin, magnetite, and albumin were dissolved in water, and then, ethanol was added dropwise under constant shaking at room temperature. To cross-link and stabilize the nanoparticles, glutaraldehyde was added to the mixture. After 24-h reaction time, nanoparticles were purified and washed with water by centrifugation. M-DOX-BSA-NPs were characterized with dynamic light scattering (DLS), atomic force microscopy (AFM), scanning electron microscopy (SEM), vibrometric sample magnetometer (VSM), and X-ray powder diffractometer (XRD). The obtained nanospheres were freeze-dried and stored at −20 °C until their use.

Cell cultures

PC3 (human prostate cancer cell) and A549 (adenocarcinomic human alveolar basal epithelial cell) cell lines were kindly provided from Biotechnology and Bioengineering Research and Application Centre, Izmir Institute of Technology, Turkey. The prostate cancer cells were grown in Dulbecco's modified Eagle's medium (DMEM) supplemented with 5% fetal bovine serum (FBS) and 1% gentamicin sulfate, and lung cancer cells were grown in Roswell Park Memorial Institute-1640 (RPMI-1640) growth medium containing 10% fetal bovine serum (FBS) and 1% gentamicin sulfate at 37 °C in 5% CO_2. Medium was refreshed every 3 days. All nanoparticles were dissolved in DMSO, and doxorubicin was dissolved in PBS before all the analyses.

In vitro *cytotoxicity assessments*

The cytotoxicity of various concentrations of the albumin nanoparticles (BSA-NPs), magnetic albumin nanoparticles (M-BSA-NPs), DOX, DOX-incorporated BSA nanoparticles (DOX-BSA-NPs), DOX-loaded magnetic BSA nanoparticles (M-DOX-BSA-NPs) on cancer cells was determined using the MTT (3-(4,5-Dimethylthiazol-2-yl)-2,5-diphenyltetrazolium bromide) assay. MTT, a yellow tetrazole, is reduced to purple formazan in living cell's mitochondria (9). The resulting formazan crystals were dissolved in DMSO. The absorbance of this solution can be quantified at 570 nm spectrophotometrically. This reduction only occurs if mitochondrial reductase enzymes are active; thus, conversion is directly related to the number of viable cells.

MTT-based *in vitro* cytotoxicity assay was performed to investigate and compare the effects of free DOX, DOX-BSA-NPs, M-DOX-BSA-NPs, BSA-NPs, and M-BSA-NP against PC3 and A549 cells according to the method described by Yamada *et al.* (10). PC3 and A549 cells were inoculated in 96-well plates at a density of 1×10^4 cells/mL and incubated for 24 h. DOX, DOX-loaded and unloaded nanocarriers that have a concentration range between 0.02 and 50 μM (for DOX containing formulations means DOX concentrations in the formulation) were added to cells and incubated for 48 h. Thereafter, 100 μg/mL MTT was added to cells, and cells were incubated for an additional 4 h at 37 °C. After that, the growth medium was removed, and 100 mL DMSO was added to each well to ensure solubilization of formazan crystals. Finally, the absorbance was determined using plate reader at a wavelength of 540 nm. Each experiment was assayed three times in triplicate. As using 'GraphPad Prism 5' software program, IC50 values (the concentration of drug that inhibits 50% of cell proliferation as compared to untreated control) of each compound were calculated. Three independent assays were repeated (n = 9).

For the visualization of cells treated with DOX and M-DOX-BSA-NPs, optical microscopy was used. PC3 and A549 cells were inoculated in 96-well plates. After waiting overnight, 1 μM free DOX and M-DOX-BSA-NPs was added into wells and incubated for 48 h. A control group of cells that was not treated with any of the drug formulations was also prepared. After incubation, they were examined using optical microscopy (Olympus-CKX41, Tokyo, Japan).

Flow cytometry analysis for apoptosis determination

To investigate the apoptotic effects of free DOX and M-DOX-BSA-NPs against PC3 and A549 cell lines, Annexin V-FITC detection kit was used. Cells (1×10^5/well) were inoculated in a 6-well plate in 1.80 mL growth medium and incubated at 37 °C in 5% CO_2 for 24 h as described in an earlier study (11). After incubation, 20 μL of free DOX and M-DOX-BSA-NPs, which is dissolved in PBS and DMSO, respectively, was added, and cells were incubated at 37 °C in 5% CO_2. Final concentrations of each drug formulation were 1–1000 nM. Untreated cells were used as a control group. At the end of 48 h, trypsin was added to cells and cells were centrifuged for 5 min. The pellet was washed with PBS. After that, the pellet was resuspended in 200 μL of binding buffer and 2 μL of annexin V-FITC, and propidium iodide (PI) was added. The stained cells were incubated for 15 min. at room temperature (25 °C). Finally, the mixture was subjected to flow cytometer (Facsanto; Beckton Dickinson, San Jose, CA, USA) analysis.

Cell cycle analysis

To determine the cell cycle effects of the free DOX and M-DOX-BSA-NPs against PC3 and A549 cells, these drugs

were tested by PI staining. Cells (5×10^5/well) were inoculated in a 6-well plate in 1.80 mL growth medium and incubated at 37 °C in 5% CO_2 for 24 h. After the incubation period, 20 μL of free DOX and M-DOX-BSA-NPs dissolved in PBS and DMSO, respectively, at a concentration range between 1 and 1000 nM. Cells were incubated at 37 °C in 5% CO_2 for 48 h, and untreated cells were used as a control group. Cells were then centrifuged at 280 × *g* for 10 min. The supernatant was discarded, and the pellet was used in the following steps. After washing with PBS, the pellet was suspended in 1 mL PBS and fixed by adding 4 mL ethanol slowly over an ice bath. The cell suspension was centrifuged at 1200 rpm for 10 min at 4 °C. Pellet was resuspended in 200 μL of 0.1% Triton-X-100 in PBS. RNAse A (200 μg/mL, 20 μL) was added to cell suspension, and cells were incubated in 37 °C in 5% CO_2 for 30 min. Twenty microliter of PI (1 mg/mL) was added and incubated at room temperature for 15 min. The cell cycle distribution was determined by flow cytometer, and data were analyzed by ModFit software.

Nanoparticles cellular uptake

Cellular uptake of M-DOX-BSA-NPs was investigated by spin-disk confocal microscopy (Andor Technology Spinning Disc Confocal Microscopy). Firstly, lamelle was placed in a 6-well plate, and then PC3 and A549 cells were inoculated in 2 mL growth medium and allowed to adhere for 24 h. The cell growth medium was changed with 2 mL of fresh medium containing 1 μM M-DOX-BSA-NPs. After 2 h, lamelle was carefully taken and fixed on lame. Finally, the lame was examined using spin-disk confocal microscopy.

Results and Discussion

Synthesis and characterization of nanoparticles

For the nanoparticle preparation, the desolvation method was used as it simple and the resulting particles can be recovered easily. The obtained particles are in range of acceptable nanometer size by this method compared to those synthesized using the emulsion techniques (12).

In albumin nanoparticles, doxorubicin can be entrapped via the combination of hydrophobic and ionic interactions (between $-NH_3^+$ of DOX and $-COO^-$ of albumin) and chemical attachment through glutaraldehyde (13). To provide magnetic targeting with nanoparticles, Fe_3O_4 was added to the mixture during nanoparticle preparation. Iron oxide MNPs, such as magnetite Fe_3O_4 or its oxidized and more stable form of maghemite γ-Fe_2O_3, are superior to other metal oxide nanoparticles for their biocompatibility and stability and are, by far, the most commonly employed MNPs for biomedical applications (14).

Hydrodynamic diameter of obtained nanoparticles was about 210 nm. AFM image of nanoparticles has revealed to the size and spherical shape of nanoparticles. Magnetization value of M-DOX-BSA-NPs was found experimentally 2.5 emu/g at room temperature when 500 G of magnetic field was applied. XRD pattern analysis also has confirmed Fe_3O_4 structure in albumin nanoparticles (5). These data have demonstrated that M-DOX-BSA-NPs are responsive to the magnetic field and have ideal properties as a drug carrier.

In vitro *cytotoxicity assessments*

The cytotoxicity of BSA-NPs, M-BSA-NPs, DOX, DOX-BSA-NPs, M-DOX-BSA-NPs at various concentrations (0.02–50 μM) against PC3 and A549 cell lines was investigated. It was expected that the unloaded BSA-NPs or M-BSA-NPs would not show toxic effect on both cancer cell lines as they are biocompatible. Viability of both cells was approximately 100% (data not shown). Similar results were obtained in other reports described by Li *et al.*, Quan *et al.*, and Shen *et al.*, (15–17). When DOX, DOX-BSA-NPs, and M-DOX-BSA-NPs were applied on PC3 and A549 cells, cell viability decreased with increasing drug concentration. On the other hand, DOX-carrying nanoparticles showed concentration-dependent inhibitory effects on cell viability, a pattern that is similar to that of DOX alone. The MTT test demonstrated that there was no pharmacodynamic loss of DOX during the preparation of M-DOX-BSA-NPs; each of M-DOX-BSA-NPs and DOX had a significant inhibition effect against PC3 and A549 cells. IC_{50} values of DOX, DOX-BSA-NPs, and M-DOX-BSA-NPs for PC3 cells were 0.51, 0.14, and 0.035 μM, and IC_{50} values of DOX, DOX-BSA-NPs, and M-DOX-BSA-NPs for A549 cells were 9.13, 3.24, and 1.68 μM, respectively. Both DOX-BSA-NPs and M-DOX-BSA-NPs were more effective than free DOX in PC3 and A549 cells; however, M-DOX-BSA-NPs have more cytotoxic effect than DOX-BSA-NPs. Our results revealed that a lower concentration of M-DOX-BSA-NPs was needed to decrease viability of both PC3 and A549 cells than free DOX to induce the same effect. These findings can be defined by the combination of cellular uptake, drug resistance, and drug release in the acidic compartments. In comparison with the cell viability of two cell lines, A549 cells showed lower sensitivity to the treatment with free DOX or DOX-carrying nanoparticles. The lower sensitivity to DOX treatment was ascribed to drug sequestration by lung resistance-related protein (LRP) inside the cytoplasmic compartments (18). A similar result was obtained in an other report described by Azarmi *et al.* (19). Cellular uptake of nanoparticles and large molecules is generally accepted to be by an endocytosis mechanism through which they accumulate in the acidic compartments of early endosomes and then trafficked to the lysosomes (20). As we showed in the earlier study (5), DOX release from nanoparticles in acidic medium is faster. Therefore, we can suggest that after nanoparticles internalized into cells, DOX released from nanoparticles in the acidic intracellular organelles.

Moreover, besides the greater cytotoxicity of M-DOX-BSA-NPs than free DOX against cancer cells, the uptake into solid tumors of albumin nanoparticles may be enhanced by albondin (gp60) receptor and secreted protein, acidic, and rich in cysteine (SPARC), resulting selective accumulation (21). Albondin receptor on the endothelial cells of tumor vessels allows transcytosis of albumin across continuous endothelium, and SPARC results in accumulation of albumin within the tumor interstitium (2,22). In our drug carrier system, magnetite structure could serve as an additional targeting agent to deliver the drug to a tumoral region with the aid of external magnetic field.

To understand how these cancer cells appeared before and after treatment with free DOX and M-DOX-BSA-NPs, optical microscopy was used. DOX-treated cells were damaged, and the number of whole cells was fewer, while most of control cells were viable. After treatment with M-DOX-BSA-NPs, almost whole cells showed characteristics of apoptosis morphology. These images have confirmed the MTT results.

Flow cytometry analysis for apoptosis determination

To investigate the apoptotic effects of free DOX and M-DOX-BSA-NPs against PC-3 and A549 cells, flow cytometry-based Annexin V staining was performed. The percentage of cell phase composition was calculated and shown in Figures 1 and 2. When free doxorubicin at a concentration of 100 nM was applied on cells, nearly 30% of PC3 and 50% of A549 cells were counted as viable. Other accounted cells were in necrosis, late apoptosis, or early apoptosis phase. At the lower concentration of free DOX, most of cells were found alive. When M-DOX-BSA-NPs at a concentration of 10 nM were applied to cells, about 20% of PC3 and 70% of A549 cells were determined as alive. Both DOX and M-DOX-BSA-NPs have induced apoptotic cell death; at higher doses, necrosis could be accounted for cell death. The specific form of cell death resulting from doxorubicin treatment varies depending on the concentration of the drug, treatment duration, and specific form of cancer (23).

Briefly, a lower concentration of M-DOX-BSA-NPs was needed to decrease viability of both PC3 and A549 cells than free DOX to induce the same effect. These results confirmed cell viability percentage data based on MTT test. Flow cytometry analysis results are given in Figures 3 and 4.

Cell cycle analysis

It is known that as a result of doxorubicin action in the cell, cellular growth is inhibited at phases G_1 and G_2 (23). To investigate the cell cycle effects of free DOX and M-DOX-BSA-NPs against PC-3 and A549 cells, DOX and this compound were applied at the different concentrations (1, 10, 100, and 1000 nM), and untreated cells were used as a control group, which was analyzed using flow cytometry-based propidium iodide (PI) staining. Firstly, it was investigated for doxorubicin against PC-3 cells and obtained cell phase composition according to G2, S, and G1 phase (Figure 5). G1 phase marks the beginning of DNA synthesis, S phase is DNA replication, and G2 phase is the last phase until the cell enters mitosis. As doxorubicin affects DNA, an increase in G1 phase was expected when high concentration of doxorubicin was applied. As doxorubicin concentration was increased, G1 phase (1–1000 nM to 4.6–35.7%, respectively) was increased, but the highest doxorubicin concentration reflected an increased number of cells in S phase (57.2%). The percentage of cells in G1 phase was found to be similar to the control group (40.6%). Secondly, the effect of M-DOX-BSA-NPs was

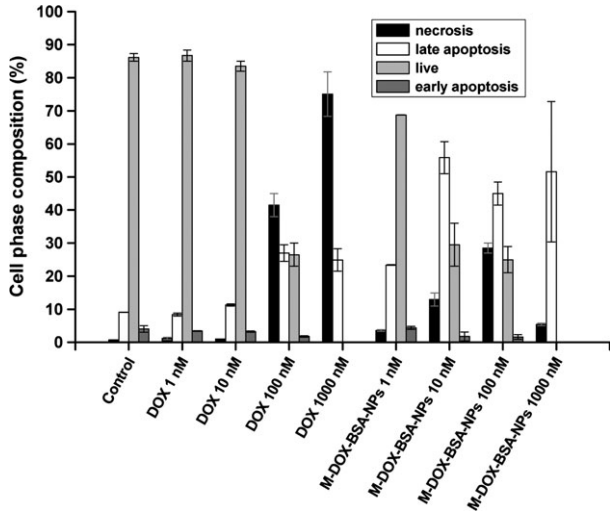

Figure 1: The phase composition percentage of PC3 cells exposed to varying concentrations of DOX and M-DOX-BSA-NPs.

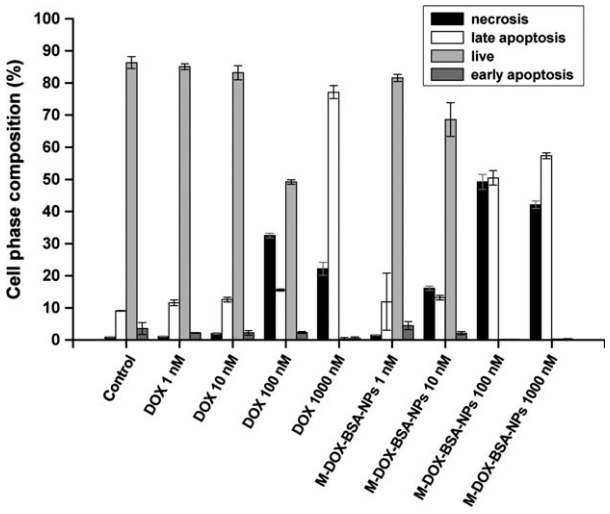

Figure 2: The phase composition percentage of A549 cells exposed to varying concentrations of DOX and M-DOX-BSA-NPs.

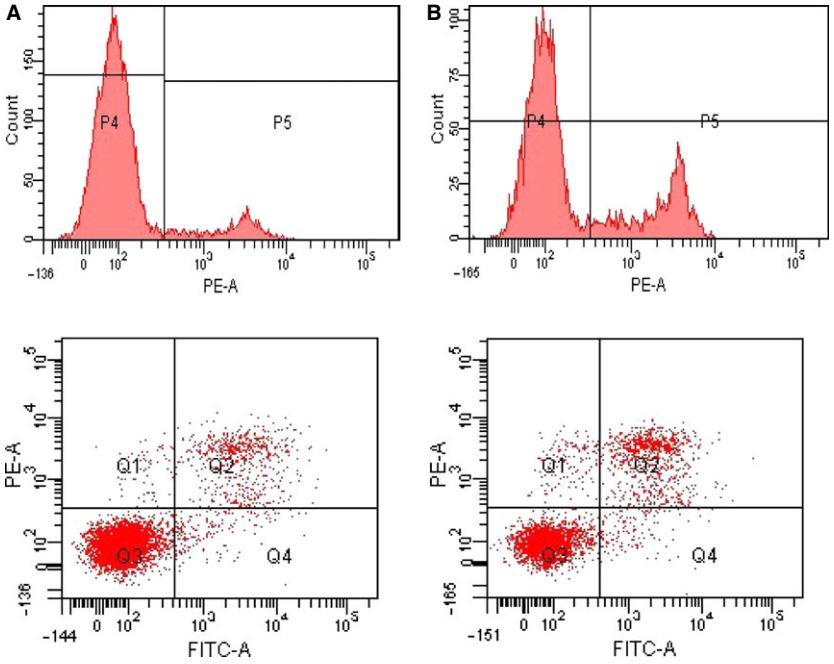

Figure 3: Flow cytometry data for PC3 cells (A) 1 nM of DOX (B) 1 nM of M-DOX-BSANPs.

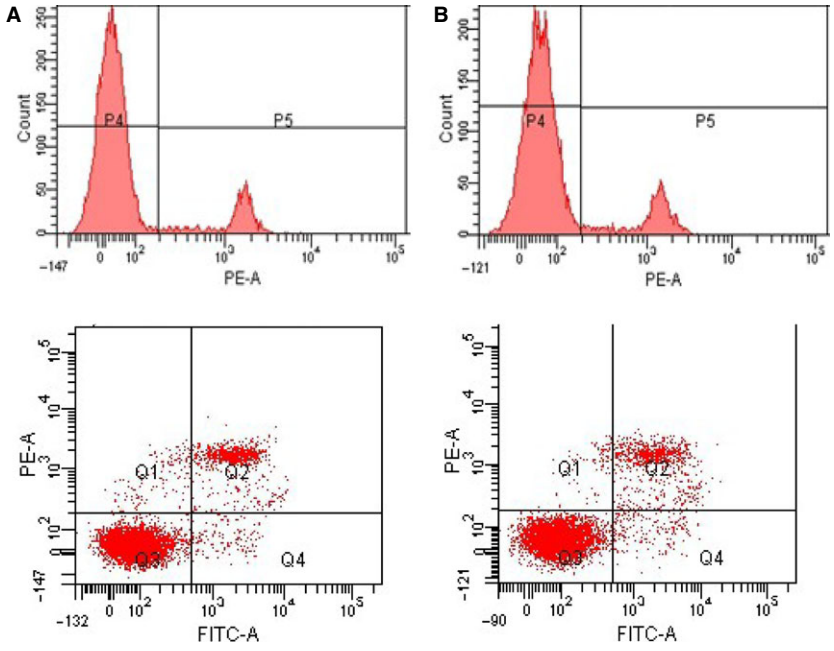

Figure 4: Flow cytometry data for A549 cells (A) 1 nM of DOX (B) 1 nM of M-DOX-BSANPs.

investigated (Figure 5). According to Figure 5, when concentration of M-DOX-BSA-NPs was increased, G1 phase (1–1000 nM to 5.5–58.2%, respectively) was increased as expected. On the other hand, when lower concentration of the compound was applied, cells in G2 phase increased. For this reason, it was thought that nanoparticles might affect G2 phase.

Next, doxorubicin was investigated against A549 cells (Figure 6). As regards to Figure 6, the percentage of cells in G1 phase was found to be similar to the control group (65.8%) at all concentration. Consequently, these concentrations of doxorubicin against A549 cells were not enough for increased G1 phase (1–1000 nM to 59.1–55.8%, respectively). Finally, the effect of M-DOX-BSA-NPs was investigated (Figure 6). The percentage of cell phase composition was calculated. As the concentration of M-DOX-BSA-NPs increased, G1 phase (1–1000 nM to 48.2–64.7%, respectively) increased as expected. However, when lower concentrations of the compound were applied,

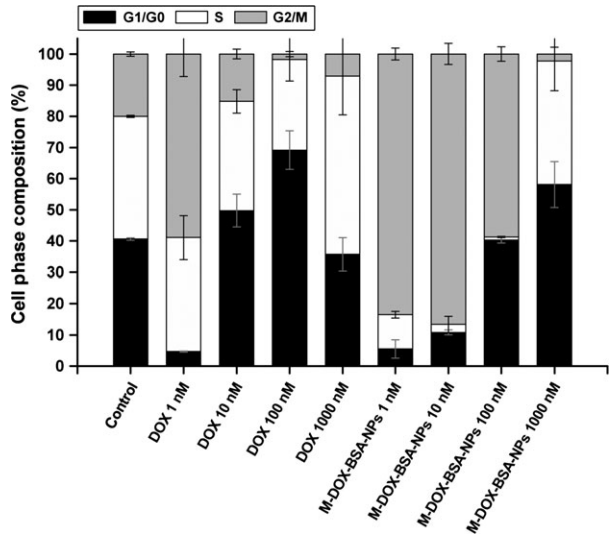

Figure 5: Effects of DOX and M-DOX-BSA-NPs with varying concentrations on cell cycle distribution of PC3 cell lines.

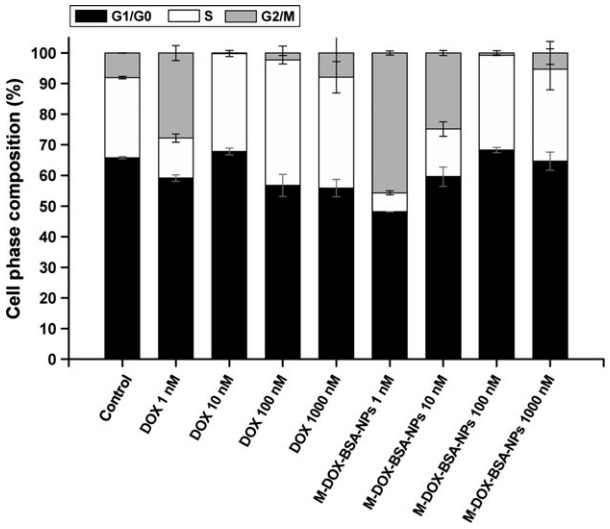

Figure 6: Effects of DOX and M-DOX-BSA-NPs with varying concentrations on cell cycle distribution of A549 cell lines.

G2 phase (1–1000 nM to 45.7–5.3%, respectively) increased as in PC-3 cell results. These results supported that nanoparticles have affected G2 phase.

Nanoparticles cellular uptake

To understand the deposition place of M-DOX-BSA-NPs in both cell types, spin-disk confocal microscopy was used (Figure 7). As doxorubicin affects DNA, it is expected that M-DOX-BSA-NPs may enter the nucleus. In fact, Figure 7B shows that M-DOX-BSA-NPs were in the PC3 cell and have reached nucleus.

On the other hand, when the same method was performed for A549 cells, it was observed that M-DOX-BSA-NPs have stayed in cell membrane and could not reach

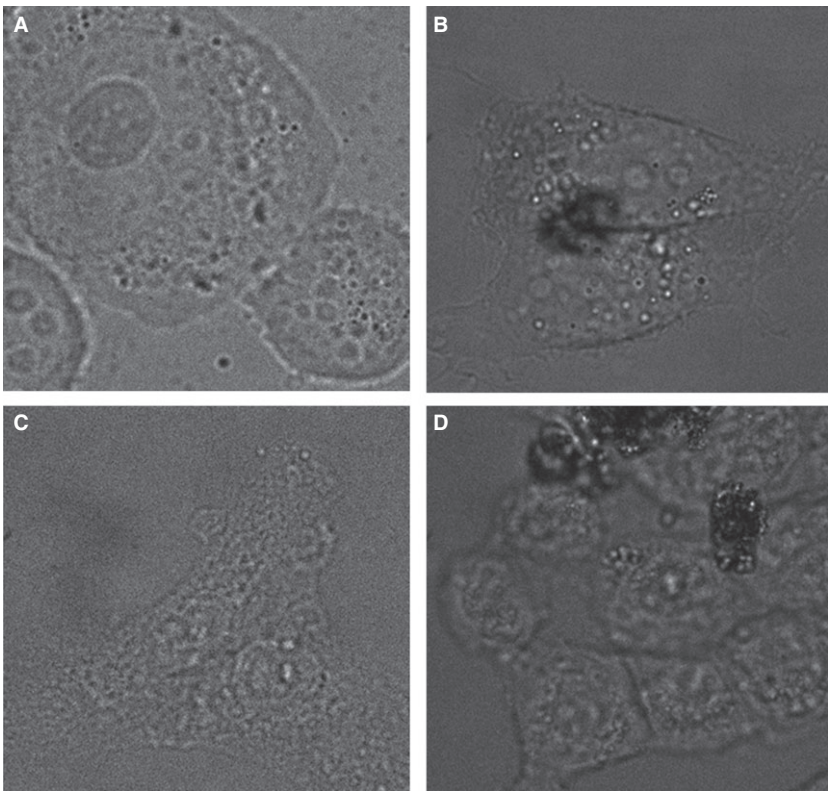

Figure 7: Spin-disk confocal microscopy images of PC3 cells treated with (A) PBS, (B) 1 μg/mL of M-DOX-BSA-NPs, and A549 cells treated with (C) PBS, (D) 1 μg/mL of M-DOXBSA-NPs.

the nucleus (Figure 7D). For this reason, it was thought that incubation time or concentration of M-DOX-BSA-NPs could not be enough for lung cancer cells. The image results indicated that M-DOX-BSA-NPs were more effective on prostate cancer cells.

Conclusion

Nanoparticles made of albumin represent a promising strategy for targeted delivery of anticancer drugs. In this study, doxorubicin-loaded magnetic albumin nanoparticles showed enhanced cytotoxic effect on both PC3 and A549 cells and nanoparticles induced more cell death than that of free doxorubicin, as determined in an apoptosis assay. The results indicated that with increasing concentrations of both formulation and free dox, the number of live cells is decreasing. However, it should be said that nanoparticles drive the cells to apoptosis in a controlled manner, and with increasing concentration, the transition between early and late apoptosis is quite mild. Cell cycle effects of free DOX and M-DOX-BSA-NPs against PC-3 and A549 cells were evaluated to determine the phase of cell cycle affected. Cell cycle analysis on both PC3 cell line and A549 cell line showed that doxorubicin-loaded magnetic albumin nanoparticles affect the G2 phase of a cell cycle. This supports the notion that these formulations affect the cell's preparation for division. Also, confocal microscopy image results demonstrated the uptake of magnetic nanospheres. According to the results, we suggest that doxorubicin-incorporated magnetic nanospheres provide many advantages as targeted drug delivery, enhanced drug killing ability and bioavailability. However, the advantages of the anticancer effects of M-DOX-BSA-NPs need *in vivo* further evaluation.

Acknowledgments

We thank Biotechnology and Bioengineering Center staff of Izmir Institute of Technology for their help and technical support.

Declaration of Interest

The authors report no conflict of interests. The authors alone are responsible for the content and writing of the paper.

References

1. Zhang L., Gu F.X., Chan J.M., Wang A.Z., Langer R.S., Farokhzad O.C. (2008) Nanoparticles in medicine: therapeutic applications and developments. Clin Pharmacol;83:761–769.
2. Elzoghby A.O., Samy W.M., Elgindy N.A. (2012a) Albumin-based nanoparticles as potential controlled release drug delivery systems. J Control Release;157:168–182.
3. Ak G., Yurt Lambrecht F., Hamarat Sanlier S. (2012a) Radiolabeling of folate targeted multifunctional conjugate with Technetium-99 m and biodistribution studies in rats. J Drug Target;20:509–514.
4. Brannon-Peppas L., Blanchette J.O. (2004) Nanoparticle and targeted systems for cancer therapy. Adv Drug Deliver Rev;56:1649–1659.
5. Ak G., Yilmaz H., Hamarat Sanlier S. (2014) Preparation of magnetically responsive albumin nanospheres and *in vitro* drug release studies. Artif Cells Nanomed Biotechnol;42:18–26.
6. Ak G., Hamarat Sanlier S. (2012b) Synthesis of folate receptor targeted and doxorubicin coupled chemotherapeutic nanoconjugate and research into its medical applications. Prep Biochem Biotech;42:551–563.
7. Lubbe A.S., Alexiou C., Bergemann C. (2001) Clinical applications of magnetic drug targeting. J Surg Res;95:200–206.
8. Corchero J.L., Villaverde A. (2009) Biomedical applications of distally controlled magnetic nanoparticles. Trends Biotechnol;27:468–476.
9. Mosmann T. (1983) Rapid colorimetric assay for cellular growth and survival: application to proliferation and cytotoxicity assay. J Immunol Methods;65:55–63.
10. Yamada A., Taniguchi Y., Kawano K., Honda T., Hattori Y., Maitani Y. (2008) Design of folate-linked liposomal doxorubicin to its antitumor effect in mice. Clin Cancer Res;14:8161–8168.
11. Blankenberg F.G., Katsikis P.D., Tait J.F., Davis R.E., Naumovski L., Ohtsuki K., Kopiwoda S., Abrams M.J., Strauss H.W. (1999) Imaging of Apoptosis (programmed cell death) with 99mTcAnnexin V. J Nucl Med;40:184–191.
12. Kumar C. (2006) Nanotechnologies for the life sciences: biological and pharmaceutical nanomaterials. In: Langer K., editor. Peptide Nanoparticles, Vol. 2. Weinheim: Wiley; p. 145–184.
13. Shen Z., Li Y., Kohama K., Oneill B., Bi J. (2011a) Improved drug targeting of cancer cells by utilizing actively targetable folic acid-conjugated albumin nanospheres. Pharmacol Res;63:51–58.
14. Shubayev V.I., Pisanic R.T., Jin S. (2009) Magnetic nanoparticles for theragnostics. Adv Drug Deliv Rev;61:467–477.
15. Li J., Chen W., Wang H., Jin C., Yu X., Lu W., Cui L., Fu D., Ni Q., Hou H. (2009) Preparation of albumin nanospheres loaded with gemcitabine and their cytotoxicity against BXPC-3 cells *in vitro*. Acta Pharmacol Sin;30:1337–1343.
16. Quan Q., Xie J., Gao H., Yang M., Zhang F., Liu G., Lin X., Wang A., Eden H.S., Lee S., Zhang G., Chen X. (2011) HSA coated iron oxide nanoparticles as drug delivery vehicles for cancer therapy. Mol Pharm;8:1669–1676.

17. Shen Z., Wei W., Tanaka H., Kohama K., Ma G., Dobashi T., Maki Y., Wang H., Bi J., Dai S. (2011b) A galactosamine-mediated drug delivery carrier for targeted liver cancer therapy. Pharmacol Res;64:410–419.
18. Meschini S., Marra M., Calcabrini A., Monti E., Gariboldi M., Dolfini E., Arancia G. (2002) Role of the lung resistance-related protein (LRP) in the drug sensitivity of cultured tumor cells. Toxicol In Vitro;16:389–398.
19. Azarmi S., Tao X., Chen H., Wang Z., Finlay W.H., Löbenberg R., Roa W.H. (2006) Formulation and cytotoxicity of doxorubicin nanoparticles carried by dry powder aerosol particles. Int J Pharm;319:155–161.
20. Talelli M., Iman M., Varkouhi A.K., Rijcken C.J.F., Schiffelers R.M., Etrych T., Ulbrich K., Van Nostrum C.F., Lammers T., Storm G., Hennink W.E. (2010) Core-crosslinked polymeric micelles with controlled release of covalently entrapped doxorubicin. Biomaterials;31:7797–7804.
21. Kratz F., Elsadek B. (2012) Clinical impact of serum proteins on drug delivery. J Control Release;161:429–445.
22. Elzoghby A.O., Samy W.M., Elgindy N.A. (2012b) Protein-based nanocarriers as promising drug and gene delivery systems. J Control Release;161:38–49.
23. Tacar O., Sriamornsak P., Dass C.R. (2012) Doxorubicin: an update on anticancer molecular action, toxicity and novel drug delivery systems. J Pharm Pharmacol;65:157–170.